Shell structure and shapes of fermion microsystems: A comparative study of ^{3}He and Na clusters

Constantine Yannouleas and Uzi Landman
School of Physics, Georgia Institute of Technology, Atlanta, Georgia 30332-0430

(Received 16 May 1996; accepted 14 August 1996)

A semiempirical shell-correction method including ellipsoidal deformations is used to determine binding energies of open-shell, unpolarized ^3He_N clusters. Shell effects, shapes, and other ground-state properties (like the chemical potential) are determined. ^3He_N clusters are found to be substantially less deformed due to their relatively high surface energy as compared to that of alkali-metal clusters (e.g., sodium clusters). As a result, the size-evolutionary patterns associated with ^3He_N clusters are significantly different than the corresponding ones for Na_N clusters. In particular, odd–even oscillations and signatures of subshell closures are absent in the case of ^3He_N clusters, while they are prominent in the case of alkali-metal clusters. © *1996 American Institute of Physics.* [S0021-9606(96)01343-8]

I. INTRODUCTION

The physics of condensed matter aggregates, such as metal clusters,[1] comprising fermionic particles has been the subject of intensifying research efforts over the past decade. In this context, analogies and methods drawn from nuclear physics proved[1–10] to be instrumental in advancing our understanding of optical excitations,[1,4,5] ground-state properties,[1–3,6–8] and fission modes[1,9,10] of such finite-size systems. In particular, it has been established that a dominant factor controlling the ground-state properties and shapes of disparate finite fermion systems (such as nuclei and simple-metal clusters, whose nature of bonding and cohesion are of very different origins with widely differing characteristic energetic and spatial scales) are the shell effects resulting from level degeneracies in conjunction with the Pauli principle (e.g., for nuclei see Ref. 11; for simple metal clusters see Ref. 8).

Among rare-gas clusters, helium clusters are unique, since they remain liquid at very low temperatures due to the importance of zero-point motion relative to the weak helium–helium interaction.[12] Thus, in contrast to heavier noble-gas clusters,[13] where geometrical packing of the atoms controls the stability properties of the ground state, helium atoms remain delocalized within the volume of the cluster, being confined by an average mean-field potential well.[14] In particular, since ^{3}He obeys fermion statistics, ^3He_N clusters may be expected to exhibit certain analogies with atomic nuclei. Indeed, such analogies, pertaining to the short-range character of both the helium–helium and nucleon–nucleon interactions, have motivated the development of theoretical Kohn–Sham-type (KS) density functional approaches to investigations of ^{3}He clusters.[14,15]

Such density functional approaches have yielded a wealth of information about some properties of ^3He_N clusters, such as density profiles, compressibility, stability, magic numbers, and shell effects of spherical closed-shell clusters. The deformations of open-shell ^3He_N clusters, however, have not been included as yet in such treatments.

The aim of the present paper is to calculate the shell effects in ^3He_N open-shell clusters in conjunction with their equilibrium deformed shapes (the influence of deformation needs to be accounted for, since it is well known that the ground state of both open-shell nuclei[11] and metallic clusters[8] does not preserve spherical symmetry). To this end, we will use a semiempirical shell-correction method (SE-SCM), which accounts for ellipsoidal (triaxial) deformations. This method was introduced[8] by us earlier in the context of studies of metal clusters, where it provided a successful interpretation of experimentally observed systematic size-evolutionary patterns of ground-state properties, such as ionization potentials, electron affinities, monomer and dimer separation energies, and fission energetics. Furthermore, we present here additional direct comparison of the oscillating part (or shell part) in the total energy of alkali-metal clusters, as well as of the second energy differences, with results extracted from experimental measurements.[16,17]

II. OUTLINE OF SEMIEMPIRICAL SHELL-CORRECTION METHOD

According to the SE-SCM, the total energy of the cluster E_T (usually also denoted[7,8] as $E_{\rm sh}$ to emphasize the fact that shell corrections have been included) is given as the sum of two terms, a liquid-drop-type smooth contribution $E_{\rm LD}$ (or $\widetilde{E}$), and a Strutinsky-type[18] shell correction $\Delta E_{\rm sh}^{\rm Str}$, namely,

$$E_T = E_{\rm LD} + \Delta E_{\rm sh}^{\rm Str}. \tag{1}$$

The general background[19] and formulation of this method for the case of neutral and charged simple-metal clusters[20] has been described in Refs. 8 and 1(a). Here we limit ourselves to a discussion of the particular features associated with each energy term which need to be considered in order to adapt the SE-SCM to the case of neutral ^{3}He clusters.

 0021-9606/96/105(19)/8734/7/$10.00

A. Liquid-drop model for deformed ^3He_N clusters

For neutral clusters, the liquid-drop model[8] (LDM) expresses the *smooth* part, $E_{\rm LD}$, of the total energy as the sum of three contributions, namely a volume, a surface, and a curvature term, i.e.,

$$E_{\rm LD}=E_{\rm vol}+E_{\rm surf}+E_{\rm curv}$$
$$=A_v\int d\tau+\sigma\int dS+A_c\int dS\kappa, \tag{2}$$

where $d\tau$ is the volume element and dS is the surface differential element. The local curvature κ is defined by the expression $\kappa=0.5(R_{\rm max}^{-1}+R_{\rm min}^{-1})$, where $R_{\rm max}$ and $R_{\rm min}$ are the two principal radii of curvature at a local point on the surface of the droplet which models the cluster. In the case of ^3He_N clusters, the corresponding coefficients have been determined by fitting[14] the total energy from KS-type calculations for closed-shell, magic spherical clusters (i.e., for $N=20$, 40, 70, 112, 168, 240, and 330, which happen to be the magic numbers corresponding to an isotropic harmonic-oscillator central potential) to the following parametrized expression as a function of the number, N, of atoms in the cluster,

$$E_{\rm LD}^{\rm sph}=\alpha_v N+\alpha_s N^{2/3}+\alpha_c N^{1/3}+\alpha_0. \tag{3}$$

The following expressions relate the coefficients A_v, σ, and A_c to the corresponding coefficients (α's) in Eq. (3),

$$A_v=\frac{3}{4\pi r_0^3}\,\alpha_v;\quad \sigma=\frac{1}{4\pi r_0^2}\,\alpha_s;\quad A_c=\frac{1}{4\pi r_0}\,\alpha_c. \tag{4}$$

In Ref. 14, the values of these coefficients were determined to be $\alpha_v=-2.49$ K, $\alpha_s=8.42$ K, $\alpha_c=4.09$ K, and $\alpha_0=-19.8$ K.

In the case of ellipsoidal shapes the areal integral and the integrated curvature can be expressed in closed analytical form with the help of the incomplete elliptic integrals $\mathscr{F}(\psi,k)$ and $\mathscr{E}(\psi,k)$ of the first and second kind,[21] respectively. Before writing the formulas, we need to introduce some notations. Volume conservation must be employed, namely,

$$a'b'c'/R_0^3=abc=1, \tag{5}$$

where R_0 is the radius of a sphere with the same volume, and $a=a'/R_0$, etc., are the dimensionless semiaxes. The eccentricities are defined through the dimensionless semiaxes as follows:

$$e_1^2=1-(c/a)^2,$$
$$e_2^2=1-(b/a)^2, \tag{6}$$
$$e_3^2=1-(c/b)^2,$$

and the semiaxes are chosen so that

$$a\geqslant b\geqslant c. \tag{7}$$

With the notation $\sin\psi=e_1$, $k_2=e_2/e_1$, and $k_3=e_3/e_1$, the relative (with respect to the spherical shape) surface and curvature energies are given[22] by

$$\frac{E_{\rm surf}^{\rm ell}}{E_{\rm surf}^{\rm sph}}=\frac{ab}{2}\left[\frac{1-e_1^2}{e_1}\,\mathscr{F}(\psi,k_3)+e_1\mathscr{E}(\psi,k_3)+c^3\right] \tag{8}$$

and

$$\frac{E_{\rm curv}^{\rm ell}}{E_{\rm curv}^{\rm sph}}=\frac{bc}{2a}\left\{1+\frac{a^3}{e_1}\left[(1-e_1^2)\mathscr{F}(\psi,k_2)+e_1^2\mathscr{E}(\psi,k_2)\right]\right\}. \tag{9}$$

B. The model external potential

Since the magic numbers of ^3He_N clusters correspond to major closures of an *isotropic* harmonic oscillator,[14,23] a natural choice for the external model potential to be used for calculating shell corrections in the SE-SCM is an *anisotropic* three-dimensional oscillator

$$H_0=-\frac{\hbar^2}{2m^*}\,\Delta+\frac{m^*}{2}\,(\omega_1^2x^2+\omega_2^2y^2+\omega_3^2z^2). \tag{10}$$

The oscillator frequencies can be related to the principal semiaxes a', b', and c' [see Eq. (5)] via the volume-conservation constraint and the requirement that the surface of the cluster is an equipotential one, namely,

$$\omega_1a'=\omega_2b'=\omega_3c'=\omega_0R_0, \tag{11}$$

where the frequency ω_0 for the spherical shape (with radius R_0) was taken according to Ref. 24 to be

$$\hbar\omega_0(N)=\frac{\hbar^2}{m^*r_0^2}\,\frac{5}{4}\,3^{1/3}N^{-1/3}=\frac{14.46}{r_0^2}\,N^{-1/3}\ \text{K Å}^2, \tag{12}$$

where $R_0=r_0N^{1/3}$. The effective mass is twice the bare ^{3}He mass,[24] i.e., $m^*=2m$. The unit radius r_0 is a slowly varying function[25] of N, namely,

$$r_0(N)=2.44+12.66N^{-2/3}-0.23N^{-1/3}\ \text{Å}. \tag{13}$$

C. Shell correction and averaging of single-particle spectra

The single-particle energies ϵ_i of the anisotropic harmonic Hamiltonian (10) are used to obtain the semiempirical Strutinsky shell correction, $\Delta E_{\rm sh}^{\rm Str}$, which is defined as follows:

$$\Delta E_{\rm sh}^{\rm Str}=\sum_i^{\rm occ}\,\epsilon_i-\widetilde{E}_{\rm sp}, \tag{14}$$

where

$$\widetilde{E}_{\rm sp}=\sum_i\,\epsilon_i\widetilde{f}_i \tag{15}$$

is the Strutinsky average of the single-particle spectrum with $\widetilde{f}_i$ being appropriate weighting factors.

Usually $\widetilde{E}_{\rm sp}$ is calculated numerically.[26] However, a variation of the numerical Strutinsky averaging method consists in using the semiclassical partition function and in expanding it in powers of $\hbar^2$. With this method, for the case of an anisotropic, fully triaxial oscillator, one finds[11,27] an analytical result, namely,

$$\widetilde{E}_{\rm sp}^{\rm osc}=\hbar(\omega_1\omega_2\omega_3)^{1/3} \times\left(\frac{1}{4}(3N)^{4/3}+\frac{1}{24}\frac{\omega_1^2+\omega_2^2+\omega_3^2}{(\omega_1\omega_2\omega_3)^{2/3}}(3N)^{2/3}\right), \quad (16)$$

where N denotes the number of ^{3}He atoms in the cluster.

In the present work, expression (16) (as modified below) will be substituted for the average part $\widetilde{E}_{\rm sp}$ in Eq. (14), while the sum $\Sigma_i^{\rm occ}\epsilon_i$ will be calculated numerically by specifying the occupied single-particle states of the oscillator represented by the Hamiltonian (10).

In the case of an isotropic oscillator, not only the smooth contribution, $\widetilde{E}_{\rm sp}^{\rm osc}$, but also the Strutinsky shell correction (14) can be specified analytically,[11] with the result

$$\Delta E_{\rm sh,0}^{\rm Str}(x)=\tfrac{1}{24}\hbar\omega_0(3N)^{2/3}[-1+12x(1-x)], \quad (17)$$

where x is the fractional filling of the highest partially filled harmonic oscillator shell. We see that for a filled shell (magic clusters having $x=0$), $\Delta E_{\rm sh,0}^{\rm Str}(0)=-\frac{1}{24}\hbar\omega_0(3N)^{2/3}$, instead of an expected vanishing value. The vanishing of the shell correction for magic (spherical) clusters originates from the fact that $E_{\rm LD}^{\rm sph}$ [see Eq. (3)] has been fitted to total energies for these clusters obtained from KS-type calculations[14] [see discussion in the context of Eq. (3)]. To adjust for this discrepancy, we add $-\Delta E_{\rm sh,0}^{\rm Str}(0)$ to $\Delta E_{\rm sh}^{\rm Str}$ calculated through Eq. (14) for the case of open-shell, as well as closed-shell clusters.

III. RESULTS

A. Cluster shapes

In this subsection, we present systematics of the ^{3}He$_N$ and Na$_N$ equilibrium triaxial shapes in the range $N\leqslant 60$. A most economical way for such a presentation is through the use of the Hill–Wheeler parameters[28] β and γ, which are related to the dimensionless semiaxes a, b, and c [see Eq. (5)] as follows:

$$a=\exp\left[\sqrt{5/(4\pi)}\beta\cos\left(\gamma-\frac{2\pi}{3}\right)\right],$$
$$b=\exp\left[\sqrt{5/(4\pi)}\beta\cos\left(\gamma+\frac{2\pi}{3}\right)\right], \quad (18)$$
$$c=\exp[\sqrt{5/(4\pi)}\beta\cos\gamma],$$

where β is unrestricted and $0\leqslant\gamma\leqslant\pi/3$. A value $\gamma\neq 0$ indicates a triaxial shape, while $\gamma=0$ corresponds to a prolate shape, and $\gamma=\pi/3$ denotes an oblate deformation. The parameter β provides a measure of the magnitude of the deformation (the origin, i.e., $\beta=0$, corresponds to a spherical shape).

Using the above definitions, the cluster potential energy surfaces (PES's) in deformation space may be easily mapped and studied. In this manner, one can analyze the topography of the PES's and identify the global minimum for each size N. The global minima are plotted in Figs. 1 and 2 for the case of ^{3}He and neutral Na clusters, respectively.

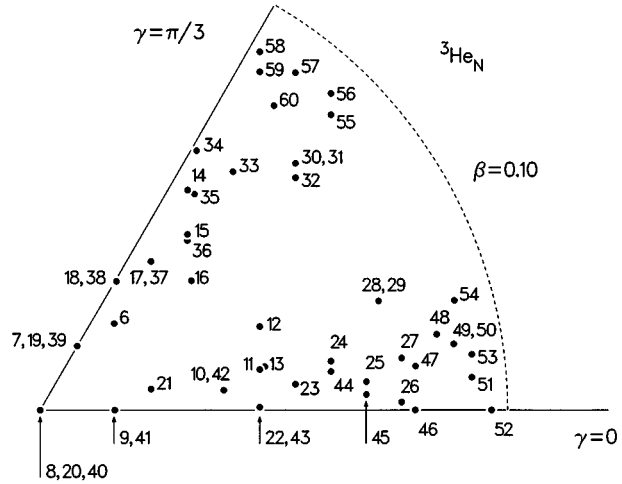

FIG. 1. The Hill–Wheeler parameters specifying the equilibrium shapes (corresponding to the global minima of the PES's) of ^{3}He$_N$ clusters according to the ellipsoidal model in the range $6\leqslant N\leqslant 60$. Observe that the dashed circle corresponds to a value of $\beta=0.10$, compared to a much larger value of $\beta=0.70$ for Na clusters (see Fig. 2).

We observe that although the γ parameter can take all possible values between 0 and $\pi/3$ in the case of ^{3}He clusters, the β parameter exhibits values noticeably smaller than corresponding values for Na clusters. As a result, the shapes of ^{3}He$_N$ clusters are much less deformed than the shapes of Na$_N$ clusters. Whether these differences in equilibrium shapes will result in marked differences in various size-evolutionary patterns, however, needs to the explicitly demonstrated through a comparison of ground-state quantities. This is done below.

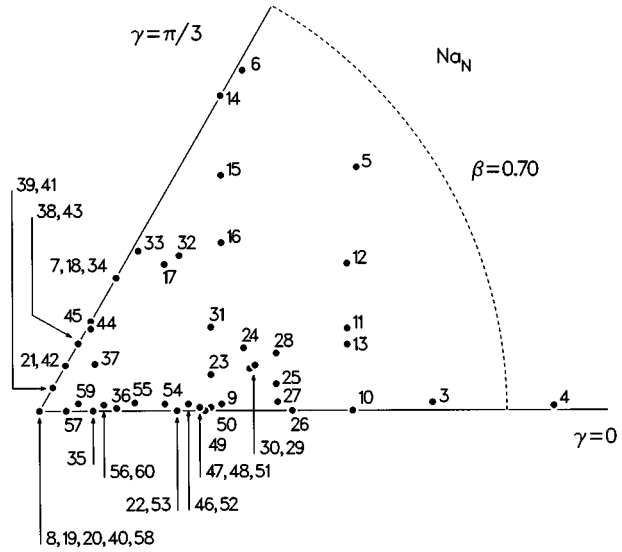

FIG. 2. The Hill–Wheeler parameters specifying the equilibrium shapes (corresponding to the global minima of the PES's) of neutral Na$_N$ clusters according to the ellipsoidal model in the range $3\leqslant N\leqslant 60$.

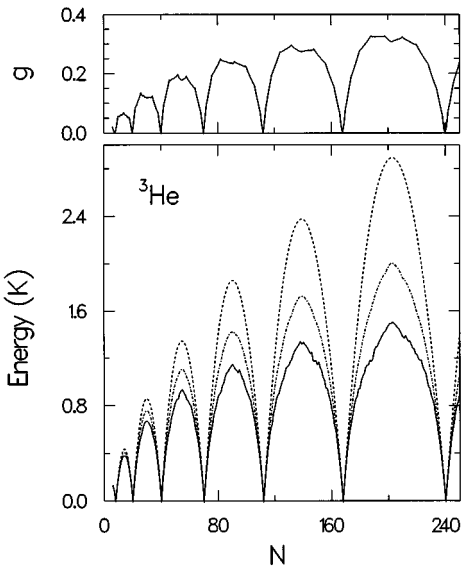

FIG. 3. Bottom panel: Theoretical SE-SCM oscillatory contributions to the total energies of triaxially deformed ^3He_N clusters in the range $6 \leqslant N \leqslant 250$. Solid line: The Strutinsky shell correction proper. Dashed-dotted line (middle line): Renormalized total energy. Dashed line: Renormalized total energy associated with corresponding spherical shapes (see the first paragraph of Sec. III B for details). Top panel: The gain factors g defined by Eq. (19). Shell closures occur at $N=8$, 20, 40, 70, 112, 168, and 240. Energies in units of degrees K.

B. Oscillatory contribution to total energies

Figures 3 and 4 display the oscillatory part of the total energies corresponding to global minima in the PES's (bottom panels) as a function of N for ^{3}He and neutral Na clusters, respectively. To provide a detailed study of this contribution, three different quantities (renormalized to the liquid drop contribution of the corresponding spherical shape) are plotted, namely, the shell correction proper, $\Delta E_{\rm sh}^{\rm Str}$ (solid curve), the renormalized total energy at the global minimum (β,γ), $\Delta E_T(\beta,\gamma)=E_T-E_{\rm LD}(\beta=0)$ (dashed-dotted curve), and their normalized total energy associated with corresponding spherical shapes, i.e., $\Delta E_T(\beta=0)=E_T(\beta=0)-E_{\rm LD}(\beta=0)=\Delta E_{\rm sh}^{\rm Str}(\beta=0)$ (dashed curve). Naturally, $\Delta E_T(\beta,\gamma)$ does not coincide with $\Delta E_{\rm sh}^{\rm Str}$ (the shell correction proper), since it also contains the liquid drop contribution due to deformation, i.e., $\Delta E_T(\beta,\gamma)=\Delta E_{\rm sh}^{\rm Str}+E_{\rm LD}(\beta,\gamma)-E_{\rm LD}(\beta=0)$. The following observations can be immediately made: The increase of the energy due to the liquid drop contribution arising from deformation [namely, $E_{\rm LD}(\beta,\gamma)-E_{\rm LD}(\beta=0)$, which is given by the difference between the dashed-dotted and the solid curves] is more important in ^{3}He clusters than in Na clusters. This is a consequence of the fact that the surface and curvature coefficients (α_s and α_c) in the case of ^{3}He clusters are, in relative terms, substantially larger than the corresponding coefficients or Na clusters (see also Sec. IV). The shell-correction curve, $\Delta E_{\rm sh}^{\rm Str}$, for sodium clusters is much ''flatter'' between magic numbers and exhibits significant fine structure. This fine structure and overall behavior are portrayed almost unaltered in the total energy curve, ΔE_T, which consequently has a profile that is substantially different from the total energy curve for spherical shapes. On the other hand, ^{3}He clusters exhibit a shell-correction-proper curve with very little structure between major shells. When the liquid drop contribution is added, the total energy curve is practically devoid of any fine structure and, apart from an overall scaling, it closely resembles the total energy curve for spherical shapes. This behavior of ΔE_T suggests that the per particle ground-state properties (like IPs, EAs, chemical potential, etc.) will exhibit rich fine structure in their size-evolutionary patterns in the case of sodium,[29] while, for ^{3}He clusters, apart from major-shell features, they will be rather monotonic (see indeed the next subsection). The net stabilization energy due to the deformation [which is the gain in energy with respect to the renormalized total energy of the corresponding spherical shapes, namely, $\Delta E_T(\beta=0)-\Delta E_T(\beta,\gamma)$] is remarkably larger in the case of Na clusters than in the case of ^{3}He clusters. To better quantify this observation, we display at the top panels of Figs. 3 and 4 the gain factors

$$g=[\Delta E_T(\beta=0)-\Delta E_T(\beta,\gamma)]/\Delta E_T(\beta=0). \tag{19}$$

We observe that, in the plotted size range, the gain factor in the middle of open shells remains most often larger than 0.5 for sodium clusters, but less than 0.35 for ^{3}He clusters. In particular, for the smaller clusters in the range $N \leqslant 70$, this factor can acquire values up to 0.70 for Na clusters, but barely up to 0.20 for ^{3}He clusters.[30]

Since no relevant experimental information exists at present for ^{3}He clusters, we restrict ourselves to confront our theoretical results for $\Delta E_T^+(\beta,\gamma)$ for singly charged sodium clusters, Na_N^+, to corresponding available experimental

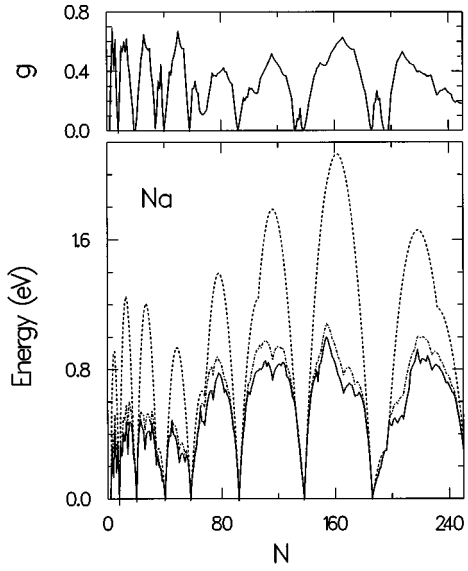

FIG. 4. Bottom panel: Theoretical SE-SCM oscillatory contributions to the total energies of triaxially deformed neutral Na_N clusters in the range $2 \leqslant N \leqslant 250$. Solid line: The Strutinsky shell correction proper. Dashed–dotted line (middle line): Renormalized total energy. Dashed line: Renormalized total energy associated with corresponding spherical shapes (see the first paragraph of Sec. III B for details). Top panel: The gain factors g defined by Eq. (19). Shell closures occur at $N=2$, 8, 20, 40, 58, 92, 138, 186, and 254. Energies in units of eV.

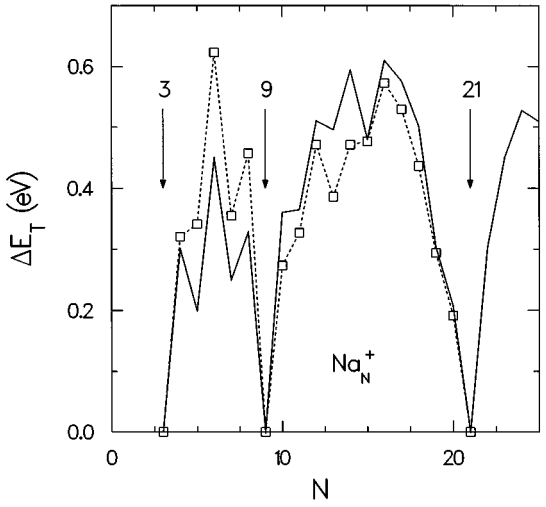

FIG. 5. Renormalized total energies (oscillatory part), $\Delta E_T = E_T - E_{\rm LD}(\beta=0)$, of small singly charged, cationic Na_N^+ clusters. Solid line: Theoretical results from the SE-SCM method with triaxial deformations. Open squares: Experimental results extracted from Ref. 16. Energies in units of eV.

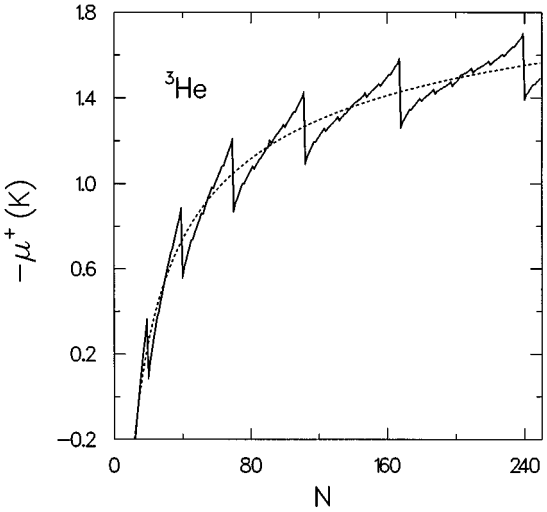

FIG. 6. Theoretical results for the chemical potential, $-\mu^+$, of ^3He_N clusters. Solid line: SE-SCM results with triaxial deformations. Dashed line: Liquid drop results for corresponding spherical shapes. Energies in units of degrees K.

results.[16] This comparison is carried out in Fig. 5, where the solid line represents our theoretical calculations and the open squares denote the experimental values.[31] The agreement between theory and experiment is remarkable, since both the experimental absolute values and fine structure (odd–even alternations and their modulations) are very well reproduced by the theory. It is worth noticing that the strong attenuation of the odd–even alternation in the range $N=16$–19 which is prominent in the experimental results is also extremely well reproduced by the theory.

C. Chemical potential of ^{3}He clusters and monomer separation energies of Na clusters

Figure 6 displays the size evolution of the chemical potential, $\mu^+ = E_T(N+1) - E_T(N)$ (solid line), of ^{3}He clusters, along with the liquid drop contribution (dashed line). Apart from the prominent features at major-shell closures, the fine structure in-between is practically insignificant.

In contrast, the monomer separation energies, $D^+_{1,N} = E^+_T(N-1) - E^+_T(N) + E_T(1)$, associated with the process $Na_N^+ \rightarrow Na_{N-1}^+ + Na$ in the case of singly charged clusters exhibit a rich fine structure between major-shell closures. This can be seen in Fig. 7(a) where the theoretical results are confronted with experimental measurements.[16] In addition to features associated with major-shell closures (i.e., for $N=9$ and 21), odd–even oscillations and subshell closures at $N=15$, 27, 31, and 35 are prominent. The agreement between theory and experiment is highly satisfactory.

Figure 7(b) displays the theoretical $D^+_{1,N}$ calculated under the restriction of spherical shapes. In this case, the disagreement with the experimental data is substantial. This illustrates further the importance of including deformations in the theoretical description of fermionic clusters before arriving at final conclusions relating to their properties [see also Refs. 8 and 1(a)].

D. Second energy differences

Another quantity which reflects shell effects in fermion microsystems is the second energy difference $\Delta_2 E = E_T(N+1) + E_T(N-1) - 2E_T(N)$. For the case of ^{3}He clusters, this quantity is displayed in Fig. 8. Again, as was the case with the chemical potential, only the features at major-shell closures are important.

The second energy differences for the case of singly charged Na_N^+ clusters are displayed in Fig. 9 (solid line) and compared to experimental results (open squares) extracted[32] form the measurements of Ref. 16. In contrast to ^{3}He clus-

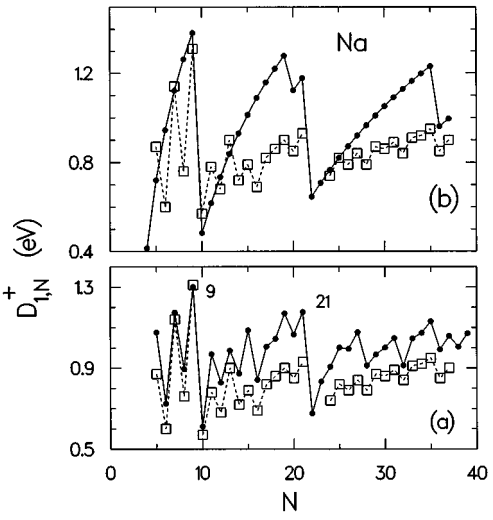

FIG. 7. Monomer separation energies, $D^+_{1,N}$, for singly charged, cationic Na_N^+ clusters in the range $5 \leqslant N \leqslant 39$. (a) Solid dots: Theoretical results derived from the SE-SCM method with triaxial deformations. Open squares: Experimental measurements from Ref. 16. (b) Solid dots: Theoretical results derived from the SE-SCM method assuming spherical shapes. Open squares: Experimental measurements from Ref. 16. Energies in units of eV.

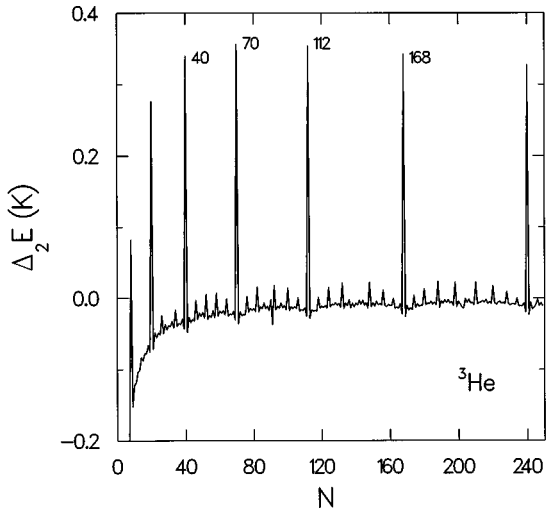

FIG. 8. Theoretical second energy differences, $\Delta_2 E$, for ^3He_N clusters derived from the SE-SCM method with triaxial deformations. Energies in units of degrees K.

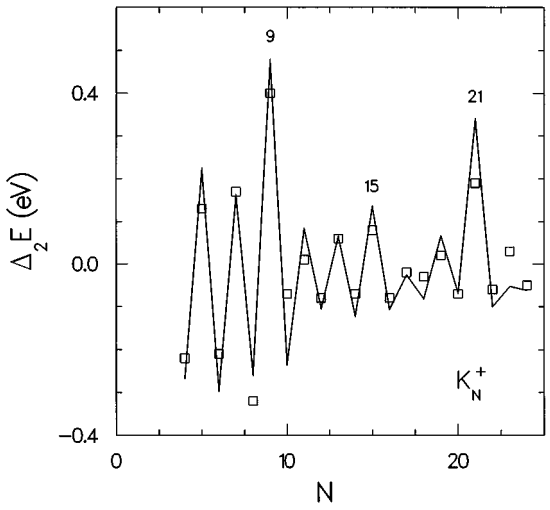

FIG. 10. Second energy differences, $\Delta_2 E$, for singly charged, cationic potassium, K_N^+, clusters. Solid line: Theoretical results derived from the SE-SCM method with triaxial deformations. Open squares: Experimental results extracted from Ref. 17. Energies in units of eV.

ters, the importance of fine structure between magic numbers is immediately noticeable. The agreement between theory and experiment is again impressive. In particular, with regard to the fine structure between magic numbers, all the odd–even alternations and their modulations (i.e., the attenuation in the range $N=16$–19 or the enhancements at the subshell closures $N=15$, 27, 31, and 35) apparent in the experimental results are very well reproduced by the theory.

The prominence of the fine structure is not limited to the case of sodium clusters, but applies to other simple metals as well. As a further example, Fig. 10 displays the second energy differences for the case of singly charged potassium clusters, K_N^+. Again our theoretical prediction (solid line) agrees remarkably well with the experimental results[17,32] (open squares). Notice that the reduction (compared to Na) in the absolute values portrayed by the experimental values is well reproduced by the theory.

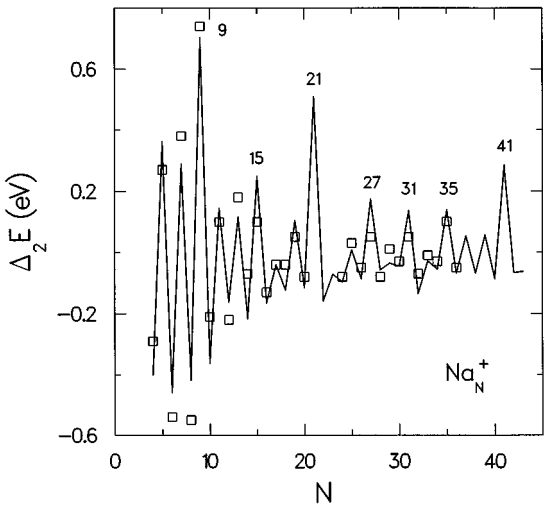

FIG. 9. Second energy differences, $\Delta_2 E$, for singly charged, cationic Na_N^+ clusters. Solid line: Theoretical results derived from the SE-SCM method with triaxial deformations. Open squares: Experimental results extracted from Ref. 16. Energies in units of eV.

IV. DISCUSSION AND CONCLUSIONS

Although both ^{3}He and Na clusters are fermionic microsystems, the size-evolutionary patterns of their ground-state properties are substantially different. Underlying the different behaviors of these two systems are the relatively high surface and curvature LDM coefficients of ^{3}He compared to those of Na clusters (for ^{3}He clusters, these coefficients are 8.42 K and 4.09 K, respectively; for sodium they are[8] 0.541 and 0.154 eV, respectively).

To provide guiding measures reflecting the different weight of these coefficients in the two systems, we compare them against the volume-energy coefficient and the energy spacing between major shells of the average oscillator potential, namely we calculate the ratios, $q_1=\alpha_s/|\alpha_v|$ and $q_2=\alpha_s/(\hbar\omega_0 N^{1/3})$ [see Eq. (12)].

$\alpha_v=-2.49$ K for ^{3}He and -2.252 eV for sodium, and thus $q_1=3.38$ and 0.24, respectively, yielding a relative ratio $q_1(^3\text{He})/q_1(\text{Na})=14$.

For Na, the effective mass m^* is equal to the bare electron mass m_e and the unit radius r_0 corresponds to the Wigner–Seitz radius $r_s=4.0$ a.u.; note that unlike r_0 for ^3He_N clusters which depends on N [see Eq. (13)], the r_s value for Na_N clusters is a constant.[33] As a result, one finds $q_2(^3\text{He})=3.47$ (assuming $r_0=2.44$ Å), $q_2(\text{Na})=0.18$, and a relative ratio $q_2(^3\text{He})/q_2(\text{Na})=19.3$. Thus the weight of the surface energy compared to the weight of the shell correction is 20 times more important in ^{3}He than it is in the case of Na clusters. This relatively much higher surface energy yields substantially less deformed ^{3}He clusters, and is the reason for the different size-evolutionary patterns between ^{3}He and Na microclusters, evaluated in this study.

ACKNOWLEDGMENTS

This research is supported by the U.S. Department of Energy (Grant No. FG05-86ER-45234). Studies were performed at the Georgia Institute of Technology Center for Computational Materials Science.

[1] For reviews, see (a) C. Yannouleas and U. Landman, in *Proceedings of the NATO Advanced Study Institute*, Course on ''Large Clusters of Atoms and Molecules,'' Erice, Italy, June 1995, NATO-ASI-Series E: Applied Sciences, Vol. 313, edited by T. P. Martin (Kluwer Academic, Dordrecht, 1996), p. 131; (b) articles in *Nuclear Aspects of Simple Metal Clusters*, edited by C. Bréchignac and Ph. Cahuzac, Comments At. Mol. Phys. **31** (1995) Nos. 3–6; (c) *Clusters of Atoms and Molecules*, edited by H. Haberland, Springer Series in Chemical Physics 52 (Springer, Berlin, 1994); (d) W. A. de Heer, Rev. Mod. Phys. **65**, 611 (1993).

[2] W. D. Knight *et al.*, Phys. Rev. Lett. **52**, 2141 (1984); K. L. Clemenger, Phys. Rev. B **32**, 1359 (1985).

[3] H. Nishioka, K. Hansen, and B. R. Mottelson, Phys. Rev. B **42**, 9377 (1990).

[4] C. Yannouleas, Chem. Phys. Lett. **193**, 587 (1992); C. Yannouleas and R. A. Broglia, Ann. Phys. (N.Y.) **217**, 105 (1992); C. Yannouleas, E. Vigezzi, and R. A. Broglia, Phys. Rev. B **47**, 9849 (1993); C. Yannouleas, F. Catara, and N. Van Giai, *ibid*. **51**, 4569 (1995).

[5] W. Ekardt, Phys. Rev. B **31**, 6360 (1985); W. Ekardt and J. M. Pacheco, *ibid*. **52**, 16 864 (1995).

[6] W. Ekardt, Phys. Rev. B **29**, 1558 (1984).

[7] C. Yannouleas and U. Landman, Phys. Rev. B **48**, 8376 (1993); Chem. Phys. Lett. **210**, 437 (1993).

[8] C. Yannouleas and U. Landman, Phys. Rev. B **51**, 1902 (1995).

[9] R. N. Barnett, U. Landman, and G. Rajagopal, Phys. Rev. Lett. **67**, 3058 (1991); C. Bréchignac, Ph. Cahuzac, F. Carlier, M. de Frutos, R. N. Barnett, and U. Landman, *ibid*. **72**, 1636 (1994).

[10] C. Yannouleas and U. Landman, J. Phys. Chem. **99**, 14577 (1995); C. Yannouleas, R. N. Barnett, and U. Landman, Comments At. Mol. Phys. **31**, 445 (1995).

[11] Å. Bohr and B. R. Mottelson, *Nuclear Structure* (Benjamin, Reading, MA, 1975), Vol. II.

[12] See articles by J. P. Toennies, K. B. Whaley, and S. Stringari, in *The Chemical Physics of Atomic and Molecular Clusters, Proceedings of the International School of Physics ''Enrico Fermi,'' 1988*, edited by G. Scoles (North-Holland, Amsterdam, 1990).

[13] H. Haberland, in Ref. 1(c), Vol. I, p. 374.

[14] S. Stringari and J. Treiner, J. Chem. Phys. **87**, 5021 (1987).

[15] S. Weisgerber and P.-G. Reinhard, Z. Phys. D **23**, 275 (1992).

[16] C. Bréchignac, Ph. Cahuzac, J. Leygnier, and J. Weiner, J. Chem. Phys. **90**, 1492 (1989).

[17] C. Bréchignac, Ph. Cahuzac, F. Carlier, M. de Frutos, and J. Leygnier, J. Chem. Phys. **93**, 7449 (1990).

[18] V. M. Strutinsky, Nucl. Phys. A **95**, 420 (1967); **122**, 1 (1968).

[19] For a microscopic local-density-approximation (LDA) foundation of the shell correction method (LDA-SCM) for metal clusters using the jellium approximation in connection with an extended Thomas–Fermi (ETF) LDA input density to a Harris-like functional, see Ref. 7. This LDA-SCM has been applied to multiply anionic metal clusters (Ref. 7) and to multiply charged fullerenes [C. Yannouleas and U. Landman, Chem. Phys. Lett. **217**, 175 (1994)].

[20] For an application of our SE-SCM to metal-cluster fission, see Ref. 10.

[21] I. S. Gradshteyn and I. M. Ryzhik, *Table of Integrals, Series, and Products* (Academic, New York, 1980), Chap. 8.11.

[22] R. W. Hasse and W. D. Myers, *Geometrical Relationships of Macroscopic Nuclear Physics* (Springer, Berlin, 1988), Chap. 6.5.

[23] A recent Kohn–Sham-type density functional approach (Ref. 15) using finite range interactions has found that above $N=168$ the shell closures deviate from those of the harmonic oscillator scheme. As was the case of metal clusters (Ref. 8) in the framework of the SE-SCM these deviations can be taken into account by adding an $\mathbf{l}^2$ perturbation to the Hamiltonian (10). Since, however, in this paper we carry out calculations for the smaller, rather than the larger, sizes, we will continue our exposition by strictly adopting the harmonic-oscillator magic numbers of Ref. 14. Apart from a rearrangement of magic numbers above 168, our conclusions concerning the contrasting behavior of size-evolutionary patterns of ^{3}He and Na clusters will not be affected.

[24] S. Stringari, in Ref. 12, p. 199.

[25] F. Castaño, M. Membrado, A. F. Pacheco, and J. Sañudo, Phys. Rev. B **48**, 12 097 (1993).

[26] J. R. Nix, Annu. Rev. Nucl. Part. Sci. **22**, 65 (1972).

[27] R. K. Bhaduri and C. K. Ross, Phys. Rev. Lett. **27**, 606 (1971).

[28] D. L. Hill and J. A. Wheeler, Phys. Rev. **89**, 1102 (1953).

[29] Indeed for the ionization potentials, electron affinities, dimer separation energies, and fission energetics of sodium clusters (as well as potassium and copper clusters), see Ref. 8.

[30] As was the case with previous investigations (Ref. 14), we find that ^{3}He clusters with $15\leqslant N\leqslant 30$ are metastable, namely they have $E_T>0$ and $\mu^+<0$. ^{3}He clusters with $N\leqslant 14$ are unstable ($E_T>0$ and $\mu^+>0$).

[31] Reference 16 has directly measured the monomer separation energies $D^+_{1,N}$ (see Sec. III C) for $N\geqslant 3$. To extract the oscillatory part ΔE^+_T of the total energy, we use the relation $-\Sigma_{j=3}^{N} D^+_{1,j}=E^+_T(N)-E^+_T(2)-(N-2)E_T(1)$ (the constant term and the term proportional to N in the right-hand-side are liquid-drop-type contributions and do not contribute to the oscillatory part). The experimental value for the monomer separation energy for $N=10$, which was not provided in Ref. 16, was specified with the help of the relation (Ref. 16), $D^+_{1,11}-D^+_{2,11}=0.75$ eV$-D^+_{1,10}$, where $D^+_{2,N}$ denotes the dimer separation energies.

[32] The second energy differences are immediately calculated from the experimental monomer separation energies listed in Refs. 16 and 17 by taking the differences $D^+_{1,N}-D^+_{1,N+1}$.

[33] The N dependence of the unit radius accounts for the fact that, within the range $6\leqslant N\leqslant 60$, the smaller $^3\mathrm{He}_N$ clusters (e.g., those with $N\leqslant 20$ in Fig. 1) are associated with an average value of β smaller than the corresponding value for larger clusters. The constancy of r_s in the case of Na_N clusters yields the opposite trend, as can be seen from Fig. 2.